Contributions to discrete adjoint method in aerodynamics for shape optimization and goal oriented mesh adaptation

HDR defense at University of Nantes

J. Peter[1]

[1]ONERA DAAA

September 25th 2020

ONERA
THE FRENCH AEROSPACE LAB

Submitted material

- Dissertation *Contributions to discrete adjoint method in aerodynamics for shape optimization and goal-oriented mesh adaptation*
- Slides and/or lecture notes of four courses about local optimization, discrete adjoint for CFD, V&V in CFD, non-intrusive UQ
- https://www.onera.fr/fr/staff/jacques-peter

- These slides follow the sections of the dissertation. The numbers in the slide titles refer to the corresponding section in the manuscript

Outline

1. Discrete gradient method for shape optimization
2. Goal-oriented mesh adaptation
3. Conclusion and perspectives

Outline

1 Discrete gradient method for shape optimization

2 Goal-oriented mesh adaptation

3 Conclusion and perspectives

§1.1 – Discrete adjoint method. Parameters

- Framework: steady state compressible flow simulation using finite-volume methods. Discrete approach for sensitivity analysis

- Notations
  - Volume mesh X, flowfield W (size n_W)
  - Wall surface mesh X_S
  - Residual R, C^1 regular w.r.t. X and W – steady state: $R(W,X)=0$
  - Vector of design parameters α (size n_α)
  - Assumption $X_S(\alpha)$ and $X(\alpha)$ are C^1 regular

- Assumption of implicit function theorem
  - $\forall\ (W_i,X_i)\ /\ R(W_i,X_i)=0 \quad (\partial R/\partial W)(W_i,X_i)\neq 0$
  - Unique steady flow corresponding to a mesh

X **volume mesh**

X_S **wall-surface mesh**

Influence of a paramter α_k **deforming** X_s **and** X

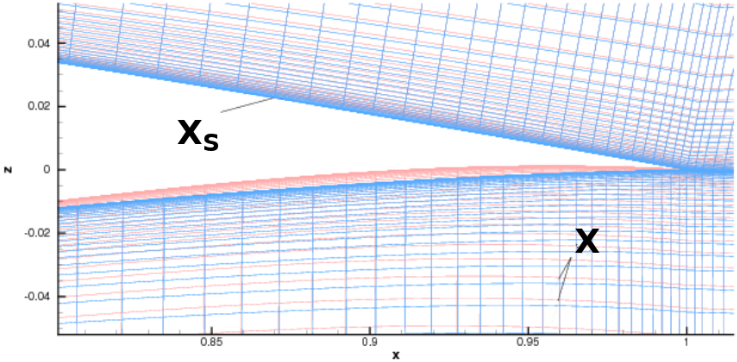

§1.1 – Discrete adjoint method. Parameters

- Using the implicit function theorem, the functions/quantities of interest (QoI) read

$$\mathcal{J}_k(\alpha) = \mathrm{J}_k(W(\alpha), X(\alpha)) \quad k \in [1, n_f] \tag{1}$$

where flowfield and volume mesh linked by flow equations

$$R(W(\alpha), X(\alpha)) = 0 \tag{2}$$

- Sensitivities $d\mathcal{J}_k/d\alpha_i \quad k \in [1, n_f] \quad i \in [1, n_\alpha]$ to be computed

- Discrete gradient computation methods
  - Finite differences – $2n_\alpha$ flow computations (non linear problems, size n_W)
  - Direct differentiation method – n_α linear systems (size n_W)
  - Adjoint vector method – n_f linear systems (size n_W)
    - Most interesting whenever $n_f << n_\alpha$ typically for external aerodynamics

§1.1 – Direct differentiation method

- Discrete equations for mechanics (set of n_W non-linear equations)

$$R(W(\alpha), X(\alpha)) = 0$$

- Differentiation with respect to α_i i $\in [1, n_\alpha]$. Derivation of n_α linear systems of size n_W

$$\frac{\partial R}{\partial W}\frac{dW}{d\alpha_i} + (\frac{\partial R}{\partial X}\frac{dX}{d\alpha_i}) = 0 \quad (3)$$

- Solving for $dW/d\alpha_i$. Calculation of sensitivities

$$\frac{d\mathcal{J}_k}{d\alpha_i} = \frac{\partial \mathrm{J}_k}{\partial X}\frac{dX}{d\alpha_i} + \frac{\partial \mathrm{J}_k}{\partial W}\frac{dW}{d\alpha_i} \quad (4)$$

§1.1 – Discrete adjoint parameter method

- Among several ways to derive the discrete adjoint equation, consistently with continuous adjoint, calculate (2)+λ^T (1) $\quad \lambda \in \mathbb{R}^{nw}$
- Vector λ defined in order to cancel the factor of the flow sensitivity $\frac{dW}{d\alpha_i}$. It appears to be associated to J_k

$$\frac{\partial \mathrm{J}_k}{\partial W} + \lambda_k^T \frac{\partial R}{\partial W} = 0 \tag{5}$$

- Calculation of derivatives

$$\nabla_\alpha \mathcal{J}_k(\alpha) = \frac{\partial \mathrm{J}_k}{\partial X}\frac{dX}{d\alpha} + \lambda_k^T (\frac{\partial R}{\partial X}\frac{dX}{d\alpha})$$

or

$$\nabla_\alpha \mathcal{J}_k(\alpha) = \left(\frac{\partial \mathrm{J}_k}{\partial X} + \Lambda_k^T \frac{\partial R}{\partial X}\right)\frac{dX}{d\alpha} \tag{6}$$

- Method with n_f and not n_α linear systems (size n_W) to solve

§1.1 Discrete adjoint method. Mesh

- Functions of interest (same mathematical assumptions)

  $J_k(X) = \mathrm{J}_k(W, X)\ k \in [1, n_f]$ for $(X, W)\ \ |\ \ R(W, X) = 0$

  $dJ_k/dX\ \ k \in [1, n_f]$ to be computed

- Discrete adjoint only. Direct differentiation counterpart of adjoint-mesh requires calculation of dW/dX which is $n_W \times n_X$ field ... not sustainable

- By identification in equation (5) or differential calculation [1]

$$\frac{dJ_k}{dX} = \frac{\partial \mathrm{J}_k}{\partial X} + \lambda_k^T \frac{\partial R}{\partial X} \qquad (7)$$

- Pros: CFD code without knowledge of parametrization, huge memory savings. Try several parametrization, move to shape derivative $(d\bar{J}_k/dX_S)$
- Cons: Matrix $(\partial R/\partial X)$ has to be explicitely computed instead of $(\partial R/\partial X)(dX/d\alpha_i)$ computable by finite differences

[1] E. Nielsen and M. Park. Using an adjoint approach to eliminate mesh sensitivities in aerodynamic design. AIAA Journal, 44(5):948953, 2006.

§1.1 Discrete adjoint method. Wall-Mesh. Shape gradient

- Take benefit of the dependency of X and X_S $D(X, X_s) = 0$ (explicit or implicit in X) to define the shape gradients (very useful for applied aerodynamics)

$$\overline{J}_k(X_S) = J_k(X) \qquad \text{where} \qquad D(X, X_s) = 0 \tag{8}$$

- Shape gradient $\mathrm{d}\overline{J}_k/dX_S$ very useful for applied aerodynamics
- Volume mesh X depending explicitely on X_S. Most efficient gradient calculation method

$$\left(\frac{\partial R}{\partial W}\right)^T \Lambda_k = -\left(\frac{\partial \mathrm{J}_k}{\partial W}\right)^T \qquad \frac{dJ_k}{dX} = \frac{\partial \mathrm{J}_k}{\partial X} + \Lambda_k^T \frac{\partial R}{\partial X} \qquad \frac{d\mathcal{J}_k}{d\alpha_l} = \left[\frac{dJ_k}{dX}\frac{dX}{dX_S}\right]\frac{dX_S}{d\alpha_l}$$

- Volume mesh depending implicitely on $D(X, X_s) = 0$ (elasticity deformation method...)

$$\left(\frac{\partial R}{\partial W}\right)^T \Lambda_k = -\left(\frac{\partial \mathrm{J}_k}{\partial W}\right)^T \qquad \left(\frac{\partial D}{\partial X}\right)^T \Gamma_k = -\left(\frac{\partial \mathrm{J}_k}{\partial X} + \Lambda^T \frac{\partial R}{\partial X}\right)^T = -\left(\frac{dJ_k}{dX}\right)^T$$

$$\frac{d\mathcal{J}_k}{d\alpha_l} = \left[\Gamma_k^T \frac{\partial D}{\partial X_S}\right]\frac{dX_S}{d\alpha_l}$$

§1.1 Discrete adjoint method. Wall-Mesh. Shape gradient

- Take benefit of the dependency of X and X_S $D(X,X_s)=0$ (explicit or implicit in X) to define the shape gradients (very useful for applied aerodynamics)

$$\overline{J}_k(X_S) = J_k(X) \qquad \text{where} \qquad D(X,X_s)=0$$

- Shape gradient $d\overline{J}_k/dX_S$ very useful for applied aerodynamics
- Volume mesh X depending explicitely on X_S. Most efficient gradient calculation method

$$\left(\frac{\partial R}{\partial W}\right)^T \Lambda_k = -\left(\frac{\partial \mathrm{J}_k}{\partial W}\right)^T \qquad \frac{dJ_k}{dX} = \frac{\partial \mathrm{J}_k}{\partial X} + \Lambda_k^T \frac{\partial R}{\partial X} \qquad \frac{d\mathcal{J}_k}{d\alpha_l} = \left[\frac{dJ_k}{dX}\,\frac{dX}{dX_S}\right]\frac{dX_S}{d\alpha_l}$$

- Volume mesh depending implicitely on $D(X,X_s)=0$ (elasticity deformation method...)

$$\left(\frac{\partial R}{\partial W}\right)^T \Lambda_k = -\left(\frac{\partial \mathrm{J}_k}{\partial W}\right)^T \qquad \left(\frac{\partial D}{\partial X}\right)^T \Gamma_k = -\left(\frac{\partial \mathrm{J}_k}{\partial X} + \Lambda^T \frac{\partial R}{\partial X}\right)^T = -\left(\frac{dJ_k}{dX}\right)^T$$

$$\frac{d\mathcal{J}_k}{d\alpha_l} = \left[\Gamma_k^T \frac{\partial D}{\partial X_S}\right]\frac{dX_S}{d\alpha_l}$$

§1.2 Implicit stages for adjoint vector calculation

- Discrete adjoint system is linear and sparse

$$\lambda_k^T \frac{\partial R}{\partial W} = -\frac{\partial J_k}{\partial W} \quad \text{or classical column vector system} \quad \frac{\partial R}{\partial W}^T \lambda_k = -\frac{\partial J_k}{\partial W}^T \quad (9)$$

- As large as the direct problem and the conditionning of the Jacobian $(\partial R/\partial W)$ is poor for (RANS) flows
- Methods without a second approximate Jacobian, just using Jacobi, Gauss-Seidel, GMRES and ILU(k) are rarely sufficient / memory-sustainable [2]

- Most often an approximate Jacobian appears either in a Fixed Point Iteration (FPI) method or in a preconditionned GMRES method.

- FPI resolutions developped by the author and coworkers

$$\left(\frac{\partial R}{\partial W}\right)^{(APP)\ T} \left(\lambda_k^{(l+1)} - \lambda_k^{(l)}\right) = -\left((\frac{\partial R}{\partial W})^T \lambda_k^{(l)} + (\frac{\partial J_k}{\partial W})^T \right) \quad (10)$$

[2] J. Peter and R.P. Dwight Numerical sensitivity analysis for aerodynamic optimization : a survey of approaches. Computers and Fluids 39 (2010)

§1.2 Implicit stages for adjoint vector calculation

- FPI resolutions developped by the author and coworkers for direct and adoint equations

$$\left(\frac{\partial R}{\partial W}\right)^{(APP)\ T}\left(\lambda_k^{(l+1)}-\lambda_k^{(l)}\right)=-\left((\frac{\partial R}{\partial W})^T\lambda_k^{(l)}+(\frac{\partial J_k}{\partial W})^T\right) \qquad (11)$$

$$\left(\frac{\partial R}{\partial W}\right)^{(APP)}\left((\frac{dW}{d\alpha_i})^{(l+1)}-(\frac{dW}{d\alpha_i})^{(l)}\right)=-\left((\frac{\partial R}{\partial W})\frac{dW}{d\alpha_i}^{(l)}+\frac{\partial R}{\partial X}\frac{dX}{d\alpha_i}\right) \qquad (12)$$

- Strong similarity with backward-Euler schemes for steady state flows

$$\left(I+\frac{\Delta t}{Vol}\frac{\partial R}{\partial W}^{(APP)}\right)\left(W^{(l+1)}-W^{(l)}\right)=-\frac{\Delta t}{Vol}R(W^{(l)}) \qquad (13)$$

- Set of implicit stages developped with J. Mayeur and F. Drullion [3] in the structured-mesh part of the *elsA* code [4]

---

[3] J. Peter and F. Drullion. Large stencil viscous flux linearization for the simulation of 3D turbulent compressible flows with backward-Euler schemes. Computers and Fluids, 36 :1005-1027, 2007.

[4] L. Cambier, S. Heib, and S. Plot. The elsA CFD software : input from research and feedback from industry. Mechanics & Industry, 14(3) :159-174, 2013.

§1.2 Implicit stages for adjoint vector calculation

- Set of implicit stages (called `LURELAX` in the framework of the *elsA* project) [5]
  - *elsA* code (FV cell-centred) Structured mesh part
  - Centred flux plus scalar (JST) or matrix dissipation
  - All terms of $(\partial R/\partial W)^{(APP)}$ are evaluated at cell-centres
  - Fourth order dissipation possibly involved in $(\partial R/\partial W)^{(APP)}$
  - Jameson-Yoon scalar approximation for convective / viscous flux balance possibly involved
  - 5-point per mesh direction viscous flux balance approximate linearization (if cell-centred gradient used in viscous fluxes)
  - Approximate resolution of the FPI linear system by 2p-LU relaxation steps
- Theoretical results of scalar linear analysis
  - (no more difference between matrix linearization and scalar approximation, scalar and matrix dissipation)
  - 5-point and 3-point per direction approximate linearization of viscous flow balance, linearizing fourth-order dissipation or not, basis unfactored scheme versus 2-step relaxation
  - Conditions of stability and conditions of convergence of relaxation iterations
  - Asset of 5-point per mesh direction viscous flux balance linearization
- Application to (RANS) external flows. AS28G wing and wing-body-pylon-nacelle

[5] J. Peter and F. Drullion. Large stencil viscous flux linearization for the simulation of 3D turbulent compressible flows with backward-Euler schemes. Computers and Fluids, 36 :1005-1027, 2007.

§1.2 Implicit stages for adjoint vector calculation

- Adaptation of `LURELAX` backward-Euler implicit stages

$$\left(I + \frac{\Delta t}{Vol}\frac{\partial R}{\partial W}^{(APP)}\right)\left(W^{(l+1)} - W^{(l)}\right) = -\frac{\Delta t}{Vol}R(W^{(l)})$$

to adjoint FPI resolution

$$\left(\frac{\partial R}{\partial W}\right)^{(APP)\ T}\left(\lambda_k^{(l+1)} - \lambda_k^{(l)}\right) = -\left(\left(\frac{\partial R}{\partial W}\right)^T \lambda_k^{(l)} + \left(\frac{\partial J_k}{\partial W}\right)^T\right)$$

- Generalization of cell-centred ∇T, ∇V... corrected at interfaces in adjacent center to center direction. No transposition of 5-point viscous stencil linearization
- Roe flux MUSCL & van Albada limiting function most often used. Matrix versions transposed (no Jameson-Yoon scalar approximation)
- The property of coefficients locality of $(\partial R/\partial W)^{(APP)}$

$$(\partial R/\partial W)^{(APP)}\delta W = \ldots F^{i-1}(W_{i-1})\delta W_{i-1} + F^{i}(W_i)\delta W_i + F^{i+1}(W_{i+1})\delta W_{i+1} + \ldots. \qquad (14)$$

can not be ensured for both direct and adjoint problem. Exact transposition of the direct matrix and recoding has been selected for adjoint

§1.3 Extension of discrete gradient to relative frame/absolute velocity

- Adaptating a (RANS) discrete adjoint framework to hovering rotor simulations
- One of the first two demonstrations with the one of NASA Langley
  - A. Dumont, A. Le Pape, J. Peter, and S. Huberson. Aerodynamic shape optimization of hovering rotors using a discrete adjoint of the Reynolds-averaged Navier-Stokes equations. Journal of the American Helicopter Society, 56(032002) :111, 2011
  - E.J. Nielsen, E.M. Lee-Rausch, W.T. Jones. Adjoint-Based Design of Rotors Using the Navier-Stokes Equations in a Noninertial Reference Frame. Journal of Aircraft. Vol. 47(2) March-April 2010
- Formulation – rotor simulation
- differentiation of R – dedicated (differentiated) post-processing – rotor parametrization – shape optimization

§1.3 Extension of discrete gradient to relative frame/absolute velocity

- Mechanical formulation. Rotating frame (or unsteady flow) but absolute velocity (or trouble at the farfield)

$$\begin{aligned}
\frac{\partial \rho}{\partial t} + div(\rho(\overline{V} - \overline{V_e})) &= 0 \\
\frac{\partial \rho \overline{V}}{\partial t} + div(\rho \overline{V} \otimes (\overline{V} - \overline{V_e}) + p\bar{\bar{I}}) &= div(\bar{\bar{\tau}} + \overline{\overline{\tau_R}}) + \bar{C} \\
\frac{\partial \rho E}{\partial t} + div(\rho E(\overline{V} - \overline{V_e}) + p\overline{V}) &= div((\bar{\bar{\tau}} + \overline{\overline{\tau_R}})\overline{V}) - div(\bar{s}) - div(\bar{s}_t)
\end{aligned}$$

$\overline{C}$ is a source term arising from the definition of velocity and frame

$$\bar{C} = -\rho\overline{\Omega} \wedge \overline{V},$$

- linearization of Roe-flux & MUSCL approach limited by Van albada function. Linearization of formulation source term. Linearization of wall boudary conditions. Linearization of farfield boundary conditions. Adapting implicit stages

- Linearization of QoI, FM, the function of merit for hovering rotors w.r.t. flow-field

§1.3 Extension of discrete gradient to relative frame/absolute velocity

- Application ERATO rotor. 4 blades. CH structured mesh
- 25 design parameters. Collective pitch and eight parameters from vectorial Bézier curves of degree 9 for changes in twist, chord and sweep in the external part of the rotor

$$\mathbf{TW}(t) = \sum_{i=0}^{i=9} \mathbf{TW_i}\ B_{i,n}(t) \qquad t = \frac{(r - 0.45\mathrm{R})}{.55\mathrm{R}} \qquad B_{i,n}(t) = \begin{pmatrix} n \\ i \end{pmatrix} t^i (1-t)^{n-i},$$

(TWi_x are fixed, $TW0_y$ fixed, the other TWy are the design parameters. $TW_y(t)$ applies at $TW_x(t)$)

- (RANS) flows $k - \omega$ model of Kok.
- Objective FM, no constraint. Discrete-adjoint gradients for non-linear conjugate gradient method. Order three polynomial interpolation for maximisation in the calculated direction
- 6,6 points increase of FM, 28 flow calculations, 7 adjoint calculations. Out of reach for finite differences (49h CPU vs 270h CPU NEC-SX8)

§1.3 Extension of discrete gradient to relative frame/absolute velocity

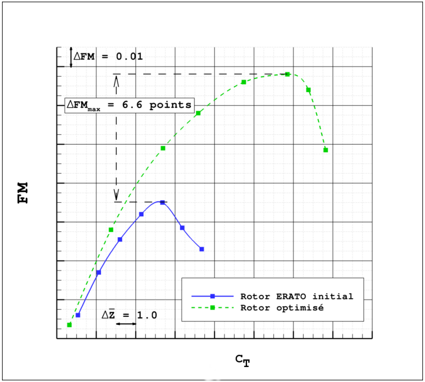

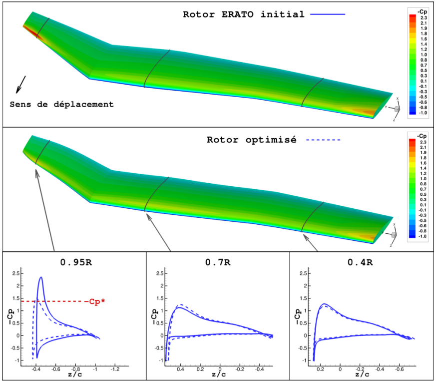

§1.4 Airfoil optimization based on shape gradient

Proposed criterion for the curvature control – Proposed smoothing method

- Suitable number of design parameters
  - Few parameters... optimal shape(s) not part of the design space
  - Numerous parameters... high frequency noise in the (shape) gradient of the QoI in particular in $d\bar{J}/dX_s$
- Optimization based on *smoothed* shape gradient or smoothed normal component $\mathcal{S}(d)$ of the shape gradient $d = (d\bar{J}/dX_s, n)$
- Shape gradient from continuous adjoint or discrete adjoint. Numerous references in 2D, few references in 3D [6]
- State of the art of implicit and explicit shape gradient presented in the manuscript
- Brief presentation of an original control of the change in curvature and an original recursive shape gradient smoothing [7] ((issue with CDf and method comparison for rank A journal publication))

[6] S. Schmidt, C. Illic, V. Schultz, N. Gauger. Three dimensional large scale aerodynamic shape optimization based on shape calculus. AIAA Journal, 51(11) :2615-2627, 2013

[7] M. Bompard, J. Peter, G. Carrier, and J.-A. Désidéri. Two-dimensional aerodynamic optimization with or without parametrization. In AIAA Paper Series, Paper 2011-3073. 2011

§1.4 Airfoil optimization based on shape gradient

Proposed criterion for the curvature control – Proposed smoothing method

- For any new proposed airfoil shape in the optim process
  - Calculate the Akima spline of the angle/Ox as a function of the arc length s
  - Differentiate the spline to get the curvature $k(s)$
  - Compute the total variation of the curvature shifted by trailing edge vs leading edge difference

$$\Psi(S) = \int_S |k'(s)| ds - |k(s_{le}) - k(s_{tu})| - |k(s_{le}) - k(s_{tl})|$$

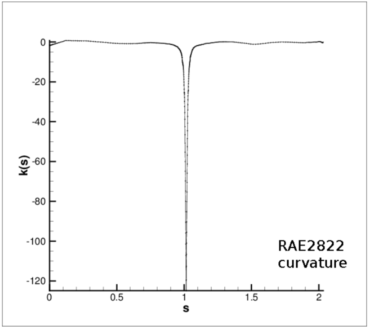

§1.4 Airfoil optimization based on shape gradient

Proposed criterion for the curvature control – Proposed smoothing method

- Criterion for curvature control
  - For any new proposed airfoil shape in the optim process compute

$$\Psi(S) = \int_S |k'(s)| ds - |k(s_{le}) - k(s_{tu})| - |k(s_{le}) - k(s_{tl})|$$

  - Proposed criterion for the acceptance of a new shape $X_S^\tau = X_S^c + \tau \mathcal{S}(d)\mathbf{n}_c$

$$\Psi(S^\tau) < q\ \Psi(S^c) \qquad (15)$$

- Smoothing method based on Dierckx's fitting (based on cubic splines)

  0 Set $l = 1$; compute $\Psi(S^c)$ (defined by X_S^c) ; set $d^0 = (d\bar{J}/dX_s^c, n_c)$; compute the descent step τ

  1 Apply Dierckx's spline interpolation with tolerance ϵ to d^{l-1} to get d^l.

  2 Compute the target airfoil $X_S^l = X_S^c + \tau\ d^l\ \mathbf{n}_c$.

  3 Compute the curvature of the Akmina's spline S^l corresponding to X_S^l ; test if $\Psi(S^l) < q\ \Psi(S^c)$. If true, stop ; otherwise restart at step 1 with $l = l + 1$.

§1.4 Airfoil optimization based on shape gradient

Proposed criterion for the curvature control – Proposed smoothing method

Example of application of the proposed smoothing.

- RAE2822. Two domains, 32832 cells. M_∞=0.73, Re=6.5 10^6 AoA=2.79^o
- *R* classical scheme differentiated in *elsA*. *X* from *Xs*, explicit distance based algebraic method of Meaux et al. $dCDw/dX_S$ suction side

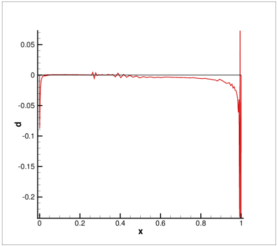

$d^0 = (dCDw/dX_S, n)$

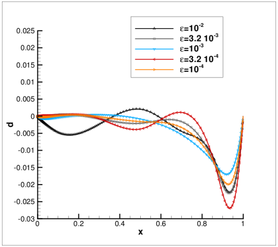

Final smoothed *d* for several ϵ

Control of $arccos(d^0, d^{final})$ stable over a range of 1 to 2 decades of ϵ. Smallest value is selected

Outline

1. Discrete gradient method for shape optimization
2. Goal-oriented mesh adaptation
3. Conclusion and perspectives

§2.1 Finite volume goal oriented mesh adaptation

Bibliography

- Well established differences between goal-oriented (G.O.) mesh adaptation and feature-based / truncation error-based / interpolation error based mesh adaptation
- G.O. mesh adaptation typically refines areas upwind the function support and more generally zones of influence with typical features for transonic (charactistics impinging shock foot) and supersonic flows (charactistics impinging trailing edge)

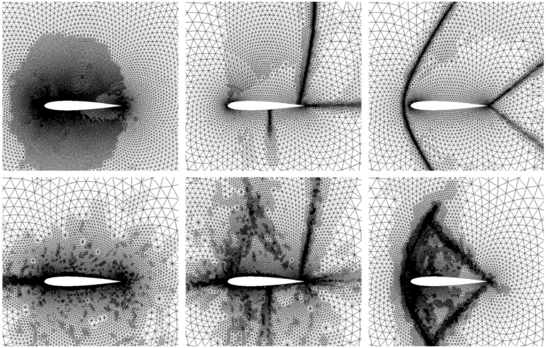

§2.1 Finite volume goal oriented mesh adaptation

Bibliography. Classical references

- Pierce and Giles' method for a linear function in an Hilbert space with a pde $Lw = f$ and corresponding adjoint pde $L^*\lambda = g$ exactly / approximately solved [8]

$$(g, w) - (g, w_h) = (g, (w - w_h)) = (L^*\lambda, (w - w_h)) = (\lambda, L(w - w_h)) = (\lambda, f - Lw_h)$$

$$(g, w) - (g, w_h) = (\lambda_h, f - Lw_h) + (\lambda - \lambda_h, f - Lw_h)$$

- Venditti and Darmofal's method, in fully discrete framework for a non-linear function [9] (various expressions of ECC)

$$\mathrm{J}_h(W_h, X_h) = \mathrm{J}_h(W_h^H, X_h) + (\Lambda_h\Big|_{W_h^H})^T R_h(W_h^H) + \mathcal{O}(||W_h - W_h^H||^2)$$

$$\mathrm{J}_h(W_h, X_h) \simeq \mathrm{J}_h(W_h^H, X_h) + \underbrace{(\Lambda_h^H)^T R_h(W_h^H)}_{computable\ \ correction} + \underbrace{((\Lambda_h\Big|_{W_h^H})^T - (\Lambda_h^H)^T) R_h(W_h^H)}_{error\ \ in\ \ computable\ \ correction\ \ (ECC)}$$

[8] M. Giles, N. Pierce. Improved lift and drag estimates using adjoint Euler equations. In AIAA Paper Series, Paper 1999-3293. 1999.

[9] D. Venditti and D. Darmofal. Grid adaptation for functional outputs : Application to twodimensional inviscid flows. Journal of Computational Physics, 176 :4069, 2002.

§2.1 Finite volume goal oriented mesh adaptation

Bibliography. Classical references

- Dwight's method for refinement based on sensitivity to the artificial dissipation of the Jameson-Schmidt-Turkel scheme [10]

$$k^2 \frac{dJ}{dk^2} + k^4 \frac{dJ}{dk^4} \text{ (error estimation on function – discussed)}$$

$$k^2 \frac{dJ}{dk_m^2} + k^4 \frac{dJ}{dk_m^4} \text{ (contribution of cell m)}$$

- Fidkowski and Roe. Physical functions with known adjoint. For inviscid flows, entropy variable = adjoint of entropy flux. Free adjoint for all G.O. methods [11]

$$\mathbf{v} = ds/dW = \left(\frac{\gamma - S}{\gamma - 1} - \frac{\rho V^2}{2p}, \frac{\rho u}{p}, \frac{\rho v}{p}, \frac{\rho w}{p}, -\frac{\rho}{p} \right)^T,$$

$$J_e = \int_{\partial\Omega} s\rho V.ndS \; .$$

[10] R. Dwight. Heuristic a posteriori estimation of error due to dissipation in finite volume schemes and application to mesh adaptation. Journal of Computational Physics, 227 :28452863, 2008.

[11] K. Fidkowski and P. Roe. An entropy approach to mesh refinement. SIAM Journal of Scientific Computing, 32(3) :1261–1287, 2010.

§2.1 Finite volume goal oriented mesh adaptation

Bibliography. Classical references

- Loseille, Dervieux, Alauzet, (Belme) method for an hybrid Finite-Volume Finite-Element scheme. [12] A priori error estimate of the goal like

$$|J(W) - J(W_h)| \leq \int_{\Omega_h} |\nabla \Lambda||\mathcal{F}(W) - \Pi_h \mathcal{F}(W)| d\Omega_h + \int_{\Gamma_h} |\Lambda||\overline{\mathcal{F}(W)} - \Pi_h \overline{\mathcal{F}(W)}| d\Omega_h$$

  Π_h linear interpolation, W exact flow, Λ exact adjoint. Solve in continuous mesh space the minimization of the upper bound

- Yano and Darmofal [13]
  - Anisotropic adaptation of simplex meshes. Minimizing an error field locally varying with the mesh (L_2 functional projection...)
  - Series of local changes to the elements. Minimizing a surrogate global model of the error using continuous mesh formalism
  - Derive a new mesh from the continuous mesh solution

---

12 A. Loseille, A. Dervieux, and F. Alauzet. Fully anisotropic mesh adaptation for 3D steady Euler equations. Journal of Computational Physics, 229 :2866-2897, 2010.

13 L. Yano and D. Darmofal. An optimization-based framework for anisotropic simplex mesh adaptation. Journal of Computational Physics, 231 :7626–7649, 2012.

§2.1 Finite volume goal oriented mesh adaptation

Bibliography. Classical references. Anisotropy

- Isotropic or anisotropic mesh refinement
- Parsing previous references with respect to anisotropy / isotropy
  - Venditti and Darmofal – Isotropic refinement for Euler flows, anistropic refinement based on the Hessian of Mach for laminar and (RANS) flows
  - Dwight – Isotropic refinement for Euler flows
  - Fidkowski et al. – All direction division of a structured anisotropic mesh (one level hanging nodes) for Euler, laminar, RANS flows
  - Loseille, Dervieux, Alauzet – intrinsically anisotropic for Euler and RANS flows
  - Yano, Darmofal – intrinsically anisotropic

§2.3 Goal oriented mesh adaptation based on dJ/dX

Motivation & intuitions

dJ/dX total derivative of QoI w.r.t. volume mesh (direct geometric dependency and global aerodynamic change reconverging flow after moving a node)

Plotting dJ/dX components and norm (1) highlights zones far from the function support (2) has strong similarities with dense zones of J-oriented refined meshes

NACA64A212 $M_\infty = 0.71$ $AoA = 2.5^o$ – left: coutour of CDw – right: coutours of $dCDw/dz$

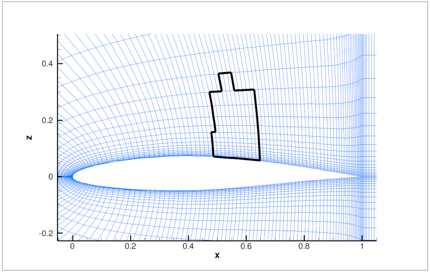

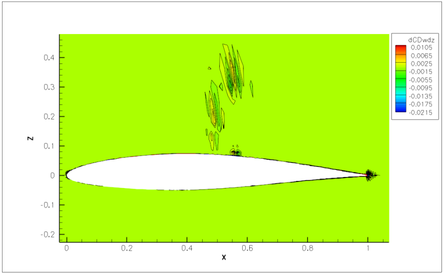

§2.3 Goal oriented mesh adaptation based on dJ/dX

Motivation & intuitions

Plotting dJ/dX components and norm (1) highlights zones far from the function support (2) has strong similarities with dense zones of J-oriented refined meshes

NACA0012 $M_\infty = 1.5$ $AoA = 1.^o$ – left: adapted mesh for CLp – right: coutours of $||dCLp/dX||$

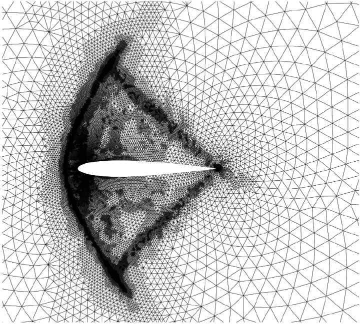

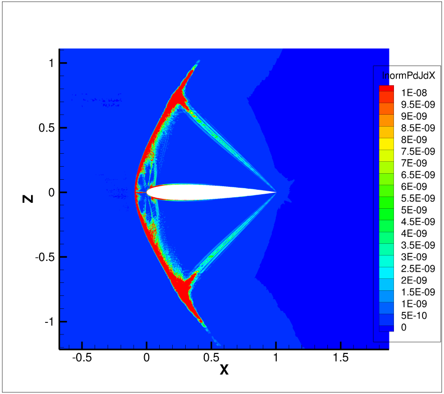

§2.3 Goal oriented mesh adaptation based on dJ/dX

Motivation & intuitions

NACA0012 $M_\infty = 0.85$ $AoA = 2.^o$ – left: adapted mesh for CLp – right: coutours of $h||\mathcal{P}(dCLp/dX)||$
$\mathcal{P}(dCLp/dX) = \mathcal{P}((\partial CLp/\partial X) + \Lambda_{CLp}(\partial R/\partial X))$

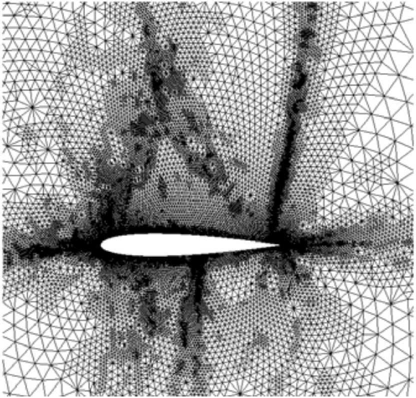

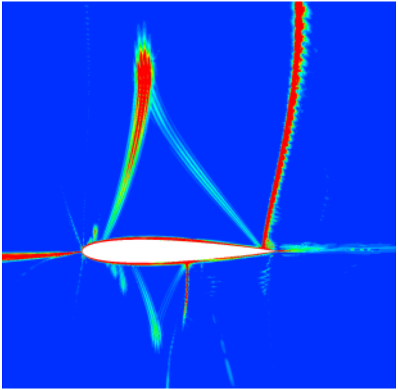

§2.3 Goal oriented mesh adaptation based on dJ/dX

Motivation & intuitions

NACA0012 $M_\infty = 0.85$ $AoA = 2.^o$ – left: adapted mesh for CLp – right: coutours of $h||\mathcal{P}(dCLp/dX)||$
$\mathcal{P}(dCLp/dX) = \mathcal{P}((\partial CLp/\partial X) + \Lambda_{CLp}(\partial R/\partial X))$

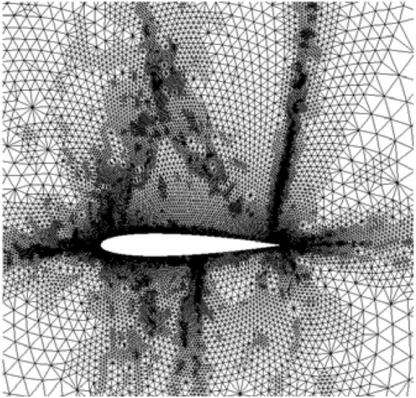

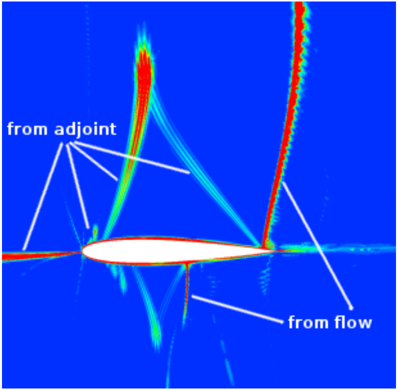

§2.3 Goal oriented mesh adaptation based on dJ/dX

Motivation & intuitions

- On regular meshes for simple Euler flows iso-$||dJ/dX||$ or $h||dJ/dX||$ very similar to mesh density of J-oriented meshes.
- From 2010 all adjoint calculations at ONERA for shape optimization use dJ/dX mode (and $d\bar{J}/dX_S$).
- Derive a goal-oriented mesh adaptation indicator not requiring two grids, not specific to a scheme or a QoI, just requiring availability of dJ/dX
- Bibliography. Other usages of dJ/dX for goal-oriented mesh adaptation ? NIA. Descent method for the mesh for a function J with known exact value or computable improved value [14] [15]
- Analysis of dJ/dX, definition a J-oriented mesh refinement indicator, simple mesh adaptations by nodes displacement and nodes addition. Assessment of families of industrial meshes. No advanced general mesh refinement capability (involving CAD, partitionning, reprojection...) has been built

[14] B. Diskin and N. Yamaleev. Grid adaptation using adjoint-based error minimization. In AIAA Paper Series, Paper 2011-3986. 2011.

[15] N. Yamaleev, B. Diskin, and K. Pathak. Error minimization via adjoint-based anistropic grid adaptation. In AIAA Paper Series, Paper 2010-4436. 2010.

§2.2 mathematical analysis of $\frac{dJ}{dX} = \frac{\partial J}{\partial X} + \Lambda^T \frac{\partial R}{\partial X}$

2D Euler flows

- Discussion requires to be very specific: 2D Euler flows, structured mesh, 4-cell flux F^R formula with S at interface as only geometric dependency. J wall integral

- $(\partial J/\partial X)$ is first-order in space
- $\Lambda^T(\partial R/\partial X)$ at least second-order in space assuming regularity of Λ and W

$$
\begin{aligned}
\Lambda^T(\partial R/\partial X_{ij}) = \sum_{k=1}^{k=4} (& (\Lambda^k_{i+1/2,j+1/2} - \Lambda^k_{i+1/2,j-1/2}) \frac{\partial F^{R,k}}{\partial S^Z}(W^L_{i+1/2,j}, W^R_{i+1/2,j}, S^X_{i+1/2,j}, S^Z_{i+1/2,j}) \\
& -(\Lambda^k_{i-1/2,j+1/2} - \Lambda^k_{i-1/2,j-1/2}) \frac{\partial F^{R,k}}{\partial S^Z}(W^R_{i-1/2,j}, W^R_{i-1/2,j}, S^X_{i-1/2,j}, S^Z_{i-1/2,j}) \\
& -(\Lambda^k_{i+1/2,j+1/2} - \Lambda^k_{i-1/2,j+1/2}) \frac{\partial F^{R,k}}{\partial S^Z}(W^L_{i,j+1/2}, W^R_{i,j+1/2}, S^X_{i,j+1/2}, S^Z_{i,j+1/2}) \\
& +(\Lambda^k_{i+1/2,j-1/2} - \Lambda^k_{i-1/2,j-1/2}) \frac{\partial F^{R,k}}{\partial S^Z}(W^L_{i,j-1/2}, W^R_{i,j-1/2}, S^X_{i,j-1/2}, S^Z_{i,j-1/2}) \quad)
\end{aligned}
$$

- numerical check of $||\Lambda^T(\partial R/\partial X)||_2$ on a hierarchy of meshes

  order$>$ 2 observed for for regular flow and no zone of numerical divergence of adjoint (subsonic flow and CD...)

  order $<<$ 2 observed in all other cases

§2.2 mathematical analysis of $\frac{dJ}{dX} = \frac{\partial J}{\partial X} + \Lambda^T \frac{\partial R}{\partial X}$

2D Euler flows

- *2D Euler flow. Structured mesh and same type of flux formula F^R as before with C^2 regularity*

  Assuming C^1 limiting fields w and λ for discrete W and Λ

  For a fixed X_{ij} outside the support of J, at the limit of fine structured meshes

$$\begin{pmatrix} \Lambda \dfrac{\partial R}{\partial x_{i,j}} \\ \Lambda \dfrac{\partial R}{\partial z_{i,j}} \end{pmatrix} = ds_{i,j} \sum_{d=1}^{4} \begin{pmatrix} \dfrac{\partial \lambda^d}{\partial z} \dfrac{\partial \mathcal{F}_Z^d}{\partial w} \dfrac{\partial w}{\partial x} - \dfrac{\partial \lambda^d}{\partial x} \dfrac{\partial \mathcal{F}_Z^d}{\partial w} \dfrac{\partial w}{\partial z} \\ -\dfrac{\partial \lambda^d}{\partial z} \dfrac{\partial \mathcal{F}_X^d}{\partial w} \dfrac{\partial w}{\partial x} + \dfrac{\partial \lambda^d}{\partial x} \dfrac{\partial \mathcal{F}_X^d}{\partial w} \dfrac{\partial w}{\partial z} \end{pmatrix} + o(ds)$$

  (Connection with Euler physical flux thanks to consistency relation)

- Very tedious calculation because of $\partial F^R / \partial X$
- Well satisfied by numerical solutions at every grid level (manuscript page 83)... but assuming λ limiting field is the solution of continuous adjoint equation, the right-hand side is zero

§2.3 First variation of J for submitted to dX

Criterion for mesh assesment and mesh refinement

- Checking dJ/dX field for usual functions and hierarchy of meshes well / not well adapted for J calculation
- Suitable refinement indicator based on first-order variation of $J(X)$ submitted to a displacement dX compliant with mesh adaptation

$$J(X + dX) - J(X) \simeq (dJ/dX).dX$$

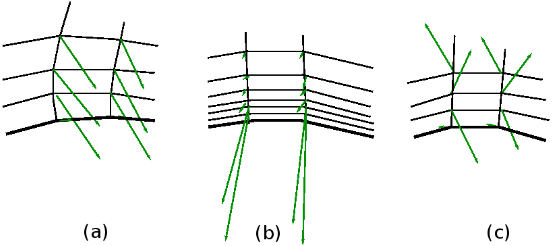

(a) (b) (c)

- Amplitude of the gradient (dJ/dX)
- Amplitude of the possible dispacement bounding dX by a local mesh size

§2.3 First variation of J for submitted to dX

Criterion for mesh assesment and mesh refinement

- Suitable refinement indicator bound of the first-order variation of $J(X)$ submitted to a displacement dX compliant with mesh adaptation

$$J(X + dX) - J(X) \simeq (dJ/dX).dX \qquad (16)$$

- Express restrictions on dX for mesh adaptation (no solid shape alteration...) through dJ/dX such that $\quad (dJ/dX).dX = \mathcal{P}(dJ/dX).dX \quad$ for admissible dX

$\mathcal{P}(dJ/dX) = dJ/dX$ Outside the support of J and solid walls contour

$\mathcal{P}(dJ/dX) = dJ/dX - (dJ/dX \cdot \vec{n})\vec{n}$

Inside the support of J, along the walls, at the outer border (normal $\vec{n}$)

$\mathcal{P}(dJ/dX) = 0$ At a corner of the support of J or at a trailing edge

- Express that only regular dX fields should be applied → spatial mean for the interior points of the domain $\overline{\mathcal{P}(dJ/dX)}$. Explicit convolution mean (Annex 4).

§2.3 First variation of J for submitted to dX

Criterion for mesh assesment and mesh refinement

- Bound of first order variation of J. For an acceptable dX (not modifying solid shape, outer boundary...)

$$J(X+dX)-J(X)\simeq(dJ/dX).dX=\mathcal{P}(dJ/dX).dX$$

$$|J(X+dX)-J(X)|\simeq|(dJ/dX).dX|\leq\sum_m||\mathcal{P}(dJ/dX_m)||\;||dX_m|| \tag{17}$$

- The final criterion $\theta[J]_m$ is obtained by fixing $||dX_m||$ to a local caracteristic mesh size, half the distance h_m to the neighboring nodes

$$\theta[J]_m=0.5||\mathcal{P}(dJ/dX_m)||h_m$$

- Expressing regularity of the realistic changes applied to the mesh

$$\overline{\theta}[J]_m=0.5||\overline{\mathcal{P}(dJ/dX)}_m||h_m$$

§2.3 First variation of J for submitted to dX

Criterion for mesh assesment and mesh refinement

- Basic criterion $\theta[J]_m$ for mesh refinement or mesh adaptation by nodes displacement

$$\theta[J]_m = 0.5||\mathcal{P}(dJ/dX_m)||h_m$$

- Expressing regularity of the realistic changes applicable to the mesh (not so usefull for mesh refinement)

$$\overline{\theta}[J]_m = 0.5||\overline{\mathcal{P}(dJ/dX)}_m||h_m$$

- Structured mesh lines/planes displacement or addition keeping the mesh lines/planes interpolated in a very fine mesh (2D and 3D – Euler and RANS flows – $\overline{\theta}$)
- Structured mesh lines/planes displacement using the mesh description by control functions in an elliptic pde (2D and 3D – Euler and RANS flows – $\overline{\theta}$ or θ)
- Unstructured mesh refinement (2D Euler – θ)
- Structured mesh "qualification" – adding $\theta[J]_m$ all over the mesh and assessing correlation with J accuracy [16]
- Structured mesh planes addition according to $\theta[J]_m$ in a multiblock structured CFD process with matching boundaries but non-matching nodes at boundaries (3D RANS flows)

[16] M. Nguyen-Dinh. Qualification des simulations numériques par adaptation anisotropique de maillages. PhD thesis, Université de Nice-Sophia Antipolis, March 2014.

§2.3 First variation of J for submitted to dX

Criterion for mesh assesment and mesh refinement

- Basic criterion $\theta[J]_m$ for mesh refinement or mesh adaptation by nodes displacement

$$\theta[J]_m = 0.5||\mathcal{P}(dJ/dX_m)||h_m$$

- Expressing regularity of the realistic changes applicable to the mesh (not so usefull for mesh refinement)

$$\overline{\theta}[J]_m = 0.5||\overline{\mathcal{P}(dJ/dX)}_m||h_m$$

- Structured mesh lines/planes displacement or addition keeping the mesh lines/planes interpolated in a very fine mesh (2D and 3D – Euler and RANS flows – $\overline{\theta}$)
- **Structured mesh lines/planes displacement using the mesh description by control functions in an elliptic pde (2D and 3D – Euler and RANS flows – $\overline{\theta}$ or θ)**
- **Unstructured mesh refinement (2D Euler – θ)**
- Structured mesh "qualification" – adding $\theta[J]_m$ all over the mesh and assessing correlation with J accuracy [17]
- Structured mesh planes addition according to $\theta[J]_m$ in a multiblock structured CFD process with matching boundaries but non-matching nodes at boundaries (3D RANS flows)

[17] M. Nguyen-Dinh. Qualification des simulations numériques par adaptation anisotropique de maillages. PhD thesis, Université de Nice-Sophia Antipolis, March 2014.

§2.4 GO mesh adaptation of 2D&3D structured meshes [18]

- Maxime-Nguyen at Airbus-F (Toulouse)
- Elliptic equation for characterization and modification of a strutured mesh
- So called-control functions of the mesh altered based on $\overline{\theta}[J]$
- 2D (RANS) flow. RAE2822 aerofoil. 513×129 mesh (ref. below §3.3.2)
  M_∞=0.725 and AoA=2.466^o, Re/m = $6.5\ 10^6$
  Three steps elliptic pde mesh adaptation based on $\overline{\theta}[CDp]$
  Improving incoming flow on the airfoil. Other aerodynamics functions improved
- 3D (RANS) flow. XRF1 wing-body. 13.5 M nodes mesh (ref. below §4.3.2 4.3.3)

[18] M. Nguyen-Dinh. Qualification des simulations numriques par adaptation anisotropique de maillages. PhD thesis, Universit de Nice-Sophia Antipolis, March 2014.

§2.4 G.O. mesh adaptation of 2D&3D structured meshes

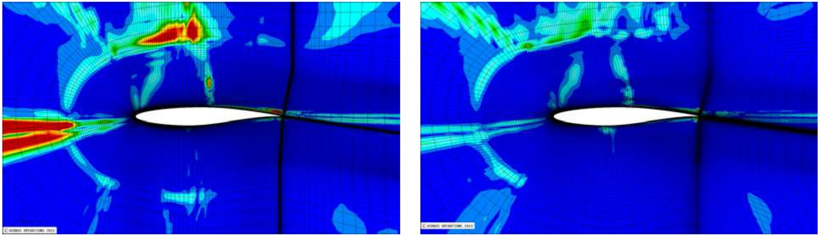

RAE2822 (RANS) flow. $\overline{\theta}[CDp]$-criterion on initial mesh and CDp-adapted mesh. (513 $\times$ 129) meshes

Mesh	CL_p	Cd ($\times 10^{-4}$)	CD_p ($\times 10^{-4}$)	CD_f($\times 10^{-4}$)
Limiting value	0.75615	118.60	60.42	58.18
Fine mesh	0.75571	118.51	60.32	58.19
Initial mesh	0.73950	123.93	62.02	61.91
Adapted mesh	0.74194	119.41	60.90	58.51

§2.5 G.O. mesh adaptation of 2D unstructured meshes

Numerical symptotic analysis of dJ/dX

- *elsA* code and adjoint module. 2D Euler flows. Roe-MUSCL scheme. $(M_\infty = 1.5, AoA = 1^o)$ $(M_\infty = 0.85, AoA = 2^o)$ $(M_\infty = 0.5, AoA = 0^o)$
- Calculating asymptotic behavior of dJ/dX is intractable due to geometric dependencies
- Using a series of embedded meshes, numerical check of global then local order of dJ/dX plotting

$$\frac{1}{n_X}\sum_{m=1}^{n_X}\|\mathcal{P}(dJ/dX_i)\| \qquad \frac{1}{ds_i}\|\mathcal{P}(dJ/dX_i)\|$$

for various mesh sizes

§2.5 G.O. mesh adaptation of 2D unstructured meshes

Plotting $1/n_X \sum_i \|\mathcal{P}(dCDp/dX_i)\|$ and $1/ds_i\|\mathcal{P}(dCDp/dX_i)\|$ for heuristic space order examination

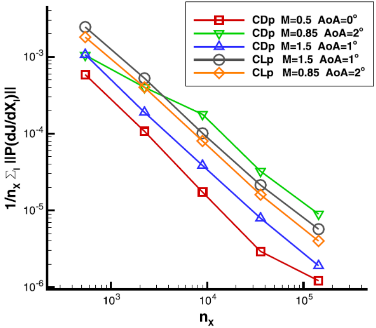

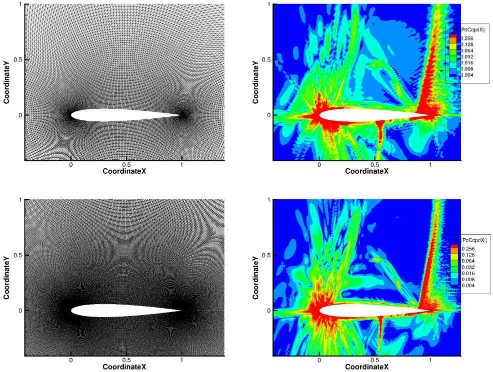

§2.5 G.O. mesh adaptation of 2D unstructured meshes [19]

Calculating local mesh size

- Applying a threshold T to θ_m field and using second order behaviour in space of dJ/dJ, h_m^{new} is derived

$$\theta_m = \left\| \mathcal{P}\left(\frac{dJ}{dX_m}\right) \right\| \frac{h_m}{2} \qquad\qquad h_m^{new} = h_m^{cur} \min\left(\left(\frac{T}{\theta_m}\right)^{1/3}, 1\right)$$

- MMG2D (INRIA) builds next mesh
- Three flow conditions. *CLp* and *CDp*
- Satisfactory convergence in functions. Expected density maps

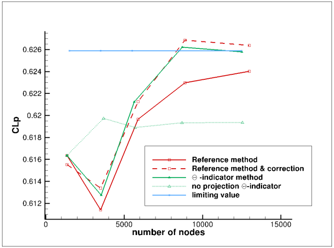

[19] G. Todarello, F. Vonck, S. Bourasseau, J. Peter, and J.-A. Désidéri. Finite-volume goal-oriented mesh-adaptation using functional derivative with respect to nodal coordinates. Journal of Computational Physics, 313 :799– 819, 2016.

Outline

1 Discrete gradient method for shape optimization

2 Goal-oriented mesh adaptation

3 Conclusion and perspectives

§3 – Perspectives

a Extension of the dJ/dX based mesh refinement to 3D unstructured meshes & (RANS) flows

- Extension of the dJ/dX based goal-oriented mesh refinement method to 3D unstructured meshes & (RANS) flows
  - Accurate dJ/dX provided by *elsA – remotorisé/sonics* for 3D (RANS) on unstructured meshes
  - Analysis of the requirements of the schemes (derivated in adjoint mode) of *elsA – remotorisé/sonics* code for the calculation of the boundary layer (BL)
  - Most probably a layer of semi-structured right-angle elements (hexaedra, prisms) close to the wall will be required for a satisfactory accuracy – see [20] (required) and [21] (not required)
  - Set the constraints of the mesh adaptation = fixed mesh in the BL, fixed number of mesh layers, fixed wall mesh

[20] M. Park, E. Lee-Rausch, and C. Rumsey. FUN3D and CFL3D computations for the first high-lift prediction workshop. In AIAA Paper Series, Paper 2011-936. 2011.

[21] L. Frazza. 3D anisotropic mesh adaptation for Reynolds averaged Navier-Stokes simulations. PhD thesis, Paris Sorbonne Université, December 2018.

§3 – Perspectives

a Extension of the dJ/dX based mesh refinement to 3D unstructured meshes & (RANS) flows

- Extension of the dJ/dX based goal-oriented mesh refinement method to 3D unstructured meshes & (RANS) flows
  - Set the constraints of the mesh adaptation = eg fixed number of mesh layers in the BL, refine the wall mesh (and consistently all righ-angle elements BL mesh), refine the external mesh
  - Accordingly define the relevant dX displacement fields. Define the corresponding projected dJ/dX field such that for relevant dX

$$(dJ/dX).dX = \mathcal{P}(dJ/dX).dX$$

  - Discuss relevance of a spatial mean for $\mathcal{P}(dJ/dX)$. Bound $|(dJ/dX).dX|$ ...

- Improving the basic features of the method
  - derive an error estimator for the method
  - derive an anisotropic version (more generally than keeping anisotropy of the BL mesh)

§3 – Perspectives

b Fundamental questions about 2D Euler lift- drag-adjoint fields

- Submitted manuscript *Analysis of finite-volume discrete adjoint fields for two-dimensional compressible Euler flows* J. Peter, F. Renac, C. Labbé. https://arxiv.org/abs/2009.07096

1 Conditions of adjoint consistency for JST scheme in 2D cell-centred FV. Discrete counterpart of continuous wall BC

2 Heuristic method to discuss adjoint consistency of discrete adjoint fields – discretizing continuous adjoint equation for discrete flow & adjoint fields

3 Examination of Rankine-Hugoniot adjoint BC for very fine grid flow & adjoint fields

4 Contribution to the mechanical asymptotic analysis of the lift- drag-adjoint behavior at the vicinity of the stagnation streamline & wall

§3 – Perspectives

b Fundamental questions about 2D Euler lift- drag-adjoint fields

- Submitted manuscript *Analysis of finite-volume discrete adjoint fields for two-dimensional compressible Euler flows* J. Peter, F. Renac, C. Labbé. https://arxiv.org/abs/2009.07096

1. Conditions of adjoint consistency for JST scheme in 2D cell-centred FV. Discrete counterpart of continuous wall BC
2. **Heuristic method to discuss adjoint consistency of discrete adjoint fields – discretizing continuous adjoint equation for discrete flow & adjoint fields**
3. **Examination of Rankine-Hugoniot adjoint BC for very fine grid flow & adjoint fields**
4. **Contribution to the mechanical asymptotic analysis of the lift- drag-adjoint behavior at the vicinity of the stagnation streamline & wall**

§3 – Perspectives

b Fundamental questions about 2D Euler lift- drag-adjoint fields

- Heuristic method to discuss adjoint consistency of discrete adjoint fields – discretizing continuous adjoint equation for discrete flow & adjoint fields. On top of theoretical results, provides info where lift- drag-ajoint is numerically diverging
- NACA0012 $M_\infty = 0.85, AoA = 2^o$. 129× 129 mesh (down) and 2049× 2049 (up). $res_{ij} = -A_{ij}^T \left(\frac{\partial \Lambda}{\partial x}\right)_{ij} - B_{ij}^T \left(\frac{\partial \Lambda}{\partial y}\right)_{ij}$

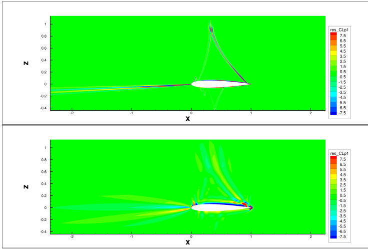

§3 – Perspectives

b Fundamental questions about 2D Euler lift- drag-adjoint fields

- C. Lozano (INTA) AIAA J (2018) *Additionally Fig [...] do hint at vanishing adjoint normal derivatives across normal shocks [...] but the evidence is not conclusive [...] For normal shocks, these relations allow to prove that normal derivatives are mostly vanishing (and continuous) across the shock* [22]
- NACA0012 $M_\infty = 0.85, AoA = 2^o$, 4097 $\times$ 4097 mesh. z-mom. residual adjoint

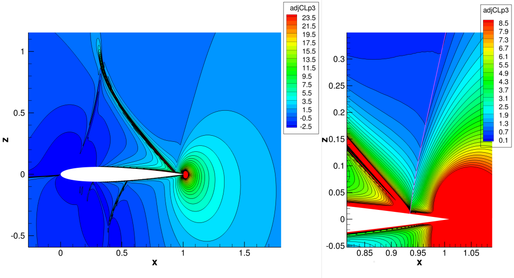

[22] C. Lozano. Singular and discontinuous solutions of the Euler adjoint equations. AIAA J. 56(11) 2018.

§3 – Perspectives

b Fundamental questions about 2D Euler lift- drag-adjoint fields

- Analysis of lift- drag-adjoint at the stagnation streamline & the wall at flow conditions where numerical divergence is observed
- Identification of the Giles-Pierce physical source term(s) involved in the numerical divergence [23]. Only the δR^4 source is involved – increase of stagnation pressure at locally constant static pressure and constant total enthalpy)
- Direct numerical analysis of the impact on the flow of a δR^4 source

[23] Giles, M. and Pierce, N. Adjoint equations in CFD: Duality, boundary conditions and solution behaviour. In AIAA Paper Series, Paper 97-1850. (1997)

§3 – Perspectives

b Fundamental questions about 2D Euler lift- drag-adjoint fields

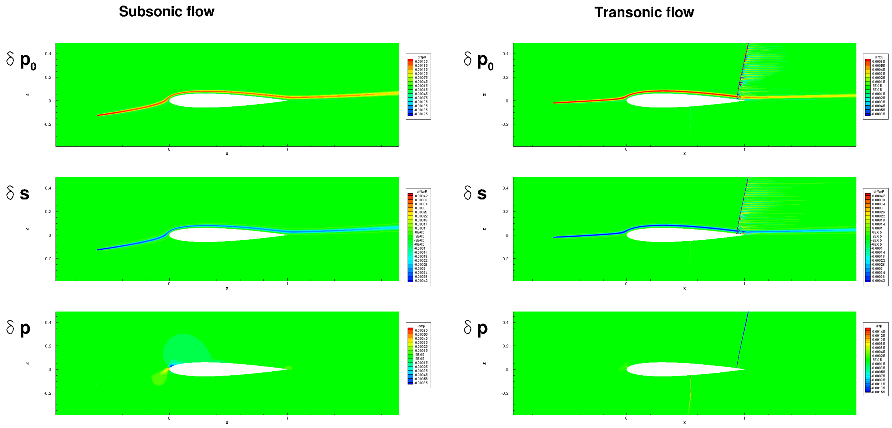

§3 – Perspectives

b Fundamental questions about 2D Euler lift- drag-adjoint fields

- Analysis of lift- drag-adjoint at the stagnation streamline & the wall at flow conditions where numerical divergence is observed
- Identification of the Giles-Pierce physical source term(s) involved in the numerical divergence. Only the δR^4 source is involved – increase of stagnation pressure at locally constant static pressure and constant total enthalpy
- Direct numerical analysis of the impact on the flow of a δR^4 source
- Convection of the δp_0, $\delta \rho_0$, δ_s created at the source. Perturbation of the static pressure field depends on the flow regime

Joint work with...

PhD students Frédérique Drullion (Embry Riddle University), Chi-Tuan Pham (EDF R&D), Meryem Marcelet (EDF production), Antoine Dumont (ONERA), Manuel Bompard (LFI Deputy at European Parlement), Maxime Nguyen-Dinh (Siemens Digital Industries), Sébastien Bourasseau (ONERA), Andrea Resmini (Renault)

MSc students Giovanni Todarello, Floris Vonck, Clément Labbé

Scientific consultant Jean-Antoine Désidéri (DR INRIA)

PhD supervisors Rémi Abgrall (Université de Zürich), Alain Lerat (ENSAM), Serge Huberson (Université de Poitiers), Dider Lucor (DR LIMSI)

Colleagues Florent Renac, Daniel Destarac, Gérald Carrier, Pierre Trontin, Arnaud Lepape, Stéphane Burguburu, Julien Mayeur, Itham Salah el Din, Sébastien Heib...

Colleagues from industry Matthieu Meaux, Renaud Sauvage, Joël Brézillon

warmly thanked for their contributions

THANK YOU FOR YOUR ATTENTION